



Water flow in *Sphagnum* hummocks: Mesocosm measurements and modelling

Jonathan S. Price*, Peter N. Whittington

Department of Geography and Environmental Management, University of Waterloo, Waterloo, ON, Canada N2L 3G1

ARTICLE INFO

Article history:

Received 25 March 2009
Received in revised form 30 November 2009
Accepted 3 December 2009

This manuscript was handled by P. Baveye
Editor-in-Chief, with the assistance of
Hans-Jörg Vogel, Associate Editor

Keywords:

Unsaturated hydraulic conductivity
Water retention
Mosses
Evaporation
RETc
Hydrus 1D

SUMMARY

The internal water fluxes within *Sphagnum* mosses critically affect the rate of evaporation and the wetness of the living upper few centimetres of moss (capitula) and the physiological processes (e.g. photosynthesis) that support them. To quantify water fluxes and stores in *Sphagnum rubellum* hummocks we used a 30 cm high column (mesocosm) of undisturbed hummock moss including the capitula, and applied a number of experiments to investigate (1) staged lowering (and raising) of the water table (*wt*) with a manometer tube; (2) pumped seepage of about 0.7 cm d^{-1} to produce a *wt* drop of 1.5 cm day^{-1} ; and (3) evaporation averaging 3.2 mm d^{-1} . Water content (θ) at saturation (θ_s) was $\sim 0.9 \text{ cm}^3 \text{ cm}^{-3}$ for all depths. Residual water content (θ_r) was $0.2 \text{ cm}^3 \text{ cm}^{-3}$ at 5 cm depth, increasing to $0.47 \text{ cm}^3 \text{ cm}^{-3}$ at 25 cm depth. Hydraulic conductivity (K) of the same top 5 cm layer ranged from $1.8 \times 10^{-3} \text{ m s}^{-1}$ at θ_s to $4 \times 10^{-8} \text{ m s}^{-1}$ at θ_r . By comparison K at 25 cm depth had a much more limited range from $2.3 \times 10^{-4} \text{ m s}^{-1}$ at θ_s to $1.1 \times 10^{-5} \text{ m s}^{-1}$ at θ_r . Staged *wt* lowering from -10 cm to -30 cm (no evaporation allowed) resulted in an abrupt change in θ that reached a stable value generally within an hour, indicating the responsiveness of moss to drainage. Staged increases also resulted in an abrupt rise in θ , but in some cases several days were required for θ to equilibrate. Pumped seepage resulted in a sequential decline of θ , requiring about 10 days for each layer to reach θ_r after the water table dropped below the sensor at the respective depths. Evaporation resulted in a similar pattern of decline but took almost three times as long. The computer simulation Hydrus 1D was used to model the fluxes and provided a good fit for the staged lowering and pumped seepage experiments, but overestimated the water loss by evaporation. We believe the reason for this is that over the longer evaporation experiment, the monolith underwent consolidation and shrinkage which reduced saturated hydraulic conductivity, thus reducing the rate of upward water flux – not accounted for in the simulation. Declining θ_s in lower layers (i.e., before pore drainage) was evidence of consolidation. The study confirms that the hydraulic structure results in a rapid transition to a low but stable water content in upper mosses when the water table falls, a low unsaturated hydraulic conductivity in such circumstances that constrains upward water flux caused by evaporation when θ_r is reached, but sustains it for a wide range of water tables. Moreover, the hydraulic parameters can be represented with the Mualem–van Genuchten approach, enabling the fluxes to be modelled in one dimension with reasonable accuracy.

© 2009 Elsevier B.V. All rights reserved.

Introduction

Sphagnum mosses are the primary peat-forming plant in northern peatlands (Kuhry and Vitt, 1996). There is a critical water requirement at the growing moss surface (capitula) to support plant metabolic processes including photosynthesis and plant matter decomposition (Clymo and Hayward, 1982; McNeil and Waddington, 2003), and evaporation (Lafleur et al., 2005) yet water transport processes in mosses, particularly in the unsaturated condition, remain an enigma because of the difficulty of measuring hydraulic properties and flows in the delicate moss matrix (Price

et al., 2008). In natural systems moss grows upon its own remains, resulting in a transition from living growing moss near the surface, to progressively more decomposed mosses with depth (Clymo, 1970, 1983, 1984; Clymo and Hayward, 1982; Hayward and Clymo, 1982; Rochefort et al., 1990), thus a concomitant range of hydraulic properties that affect water flows and stores. The peat below the lowest annual average water table is referred to as the “catotelm” (Ingram, 1978), and is characterized by relatively small average pore-diameter and low hydraulic conductivity (Hayward and Clymo, 1982). Above this, the “acrotelm” comprises plant structures ranging from relatively poorly to moderately decomposed mosses at depth, to undecomposed and living mosses near the surface (Ingram, 1978). The upper layer has a larger average pore-diameter (Rezanezhad et al., 2009) and higher saturated hydraulic

* Corresponding author. Tel.: +1 519 888 4567x35711; fax: +1 519 746 0658.
E-mail address: jsprice@uwaterloo.ca (J.S. Price).

conductivity, but when drained its poor water retention results in low unsaturated hydraulic conductivity (Price et al., 2008), thus limited ability to sustain upward water movement.

Mosses are non-vascular, thus water transport occurs primarily as capillary flow in the spaces between individual leaves and pendant branches (Hayward and Clymo, 1982), while vapour constitutes only 1% of the total flux (Price et al., 2009). Water is also held in intercellular spaces called hyaline cells, that can hold 10–20% of the sample volume's water at pressures greater than –100 cm of water (Hayward and Clymo, 1982) so that during all but the driest periods the top, growing part of the *Sphagnum* remains moist. Consequently, community architecture, which is a function of species type and water availability (Schipperges and Rydin, 1998) affects water conductance potential. For example, *Sphagnum* species in hummocks (e.g. *S. fuscum*) are smaller than hollow species (e.g. *S. magellanicum*) (Schipperges and Rydin, 1998) and have higher spatial density of capitula (Gunnarsson and Rydin, 2000) which imparts a higher water retention capacity (Luken, 1985) (see also Clymo, 1970). While the water flux dynamics of hummocks and hollows have been measured using mass balance (Yazaki et al., 2006), no rigorous attempts to numerically simulate flow phenomena has been done because reliable estimates of hydraulic parameters, especially unsaturated hydraulic conductivity, have not been available until recently (Price et al., 2008). Schouwenaars and Gosen (2007) modelled water flow in mosses re-established on cutover peat and showed that it becomes increasingly difficult to sustain a water flux to the surface (capitula) once the layer grew 5–15 cm thick. However, they also suggested that as the moss layer developed even further, water storage in the lower mosses became a source that could sustain the upward flow. While this modeling contributed to the understanding of the functioning of a regenerating layer of mosses, the absence of direct measurements of hydraulic conductivity and comparative field measurements limits its applicability and reliability.

Disturbances such as drainage (Whittington and Price, 2006) or climate shifts (Tolonen and Turunen, 1996) can profoundly alter the hydrological regime, and the ecosystem response can range from desiccation and death (Sagot and Rochefort, 1996) in the short-term, to changes in moss community composition (Strack et al., 2006) over time. Improved knowledge of the linkage between groundwater and moisture at the moss surface will allow us to better predict the response. Therefore, the overall goal of this paper is to seek a better understanding of liquid water flux in a *Sphagnum* hummock profile, through measurement and modeling. The specific objectives are to (1) characterize the hydraulic structure (water retention capacity and unsaturated hydraulic conductivity relation) of a moss profile; (2) evaluate the detailed moisture response in a moss profile under changing boundary conditions (drainage, evaporation); and (3) effectively simulate the water fluxes and stores.

Methods

Our approach was to manipulate the water table in, or water flux through, intact ~35 cm diameter monoliths of *Sphagnum rubellum* hummocks in a laboratory setting; section the profile and determine the vertical hydraulic properties; and use these measurements to specify and test a 1-dimensional mathematical model.

Sample extraction and preparation

The sample was obtained from a Southern Ontario bog (49.94°N, 80.45°W) in December (when the ground was frozen),

by cutting (with a saw) a cylindrical monolith of peat with a diameter and height of ~35 cm. The moss monolith was then placed on top of a large bucket (20 l, 30 cm diameter) and the edges of the sample trimmed so that the sample slid into the bucket, ensuring a snug fit. The sample was then returned to the laboratory, flooded with deionised water, and frozen. It was then removed from the bucket so that it could be inserted intact into a second bucket that contained a 3 cm deep layer of fine gravel base (average stone diameter ~3 mm), which distributed the hydraulic connection to a flexible manometer tube fixed to the bottom of the bucket which allowed for water table manipulation and/or drainage and rewetting. The sample was allowed to thaw and then flushed with deionized water several times. To limit all vertical moisture flow to that in the *Sphagnum* matrix, the ericaceous vegetation was clipped, with roots left in place.

Moisture content was measured with a Campbell Scientific TDR100 system with 30 cm CS-605 probes connected to a CR10x data logger. Six probes were installed horizontally into the sample at –5, –10, –15, –20 and –25 cm depths, with the sixth probe inserted on an angle from 0 to –5 cm. (the angle allowed the 30 cm long probe to obtain an average of the moisture content over the top 5 cm of the sample, arguably the most important layer for water loss. As the sample surface was not perfectly flat, obtaining reliable moisture contents in this range would be impossible as part of the probe could be exposed to the air in the middle of the sample.) Small holes were drilled into the side of bucket, and the TDR probes inserted and sealed in with General Electric Silicone II to eliminate leaks. The silicone was applied to the outside of the bucket and thus there was minimal contact with the sample. Moisture content was recorded hourly unless otherwise noted. Deionized water was used for all of the following experiments.

Bucket experiments

Experiment 1: The water table (*wt*) in the sample was adjusted to –10 cm by allowing the fully saturated sample to drain through the manometer tube until the water level in the manometer was 10 cm below the moss surface. The sample was then covered loosely to prohibit evaporation. When a stable moisture content (no discernable change over at least 12 h) was achieved in the sensors above the water table, *wt* was “instantaneously” lowered 5 cm by basal drainage using the manometer tube, to five subsequent *wt* depths (–10, –15, –20, –25 and –30 cm). The process was then reversed, and the *wt* increased to the same series of depths by connecting the flexible manometer tube to a water-filled bucket that was raised above the sample.

Experiment 2: With the *wt* at –10 cm (end of experiment 1, sample still covered), the manometer tube was connected to a VWR peristaltic variable flow mini-pump (pump I, model 3384, ultra low flow; see www.vwr.com) that generated a controlled continuous basal seepage of ~0.7 cm day⁻¹ to produce a *wt* drop of 1.5 cm day⁻¹. The *wt* was measured daily in the manometer tube.

Experiment 3: The *wt* was returned to –10 cm and the cover removed. Water loss via evaporation was monitored by periodic (~daily) weighing of the monolith. The sample was placed under grow lights (0600–1900 h) with a fan ~2 m away to increase evaporation. The experiment ended when a *wt* of –30 cm was achieved.

Hydraulic conductivity and retention

Upon completion of the experiments, the core was drained of water and frozen. The frozen core was cut into five horizontal layers ~5 cm thick centered at –5, –10, –15, –20 and –25 cm below the surface (e.g., the first was –2.5 to –7.5 cm). The 0 to –2.5 cm layer was discarded as the core did not have a perfectly flat surface and a viable sample was infeasible. The lowest layer (–27.5 to

~30 cm) was also discarded because the bottom was not perfectly flat, only 2.5 cm thick, and fine gravel had become embedded in the core. From these layers bulk density was calculated from a sub-sample of known volume using dried mass (24 h at 95 °C).

The unsaturated condition hydraulic conductivity (K) was determined on 12.7 cm dia. cores for each 5 cm layer using the apparatus described by Price et al. (2008), who provide a full description of the method and apparatus. Briefly, the core was placed between two high-flow tension disks (top and bottom) that applied suction to the core. The tension disks were constructed from 2.5 cm high by 11.4 cm diameter rings of Plexiglas sealed on one end with a 12.4 cm diameter by 0.318 cm thick disk of Plexiglas and the other with either a 25 or 35 μm NitexTM fabric that had an air-entry pressure of -40 or -35 cm, respectively. The non-Nitex side of the tension disk had a spigot that allowed a flexible tube to be attached to change the height of the in- and outflow locations from the disks. The disks were filled with water and air removed before the sample was placed between them. The outflow of the upper disk was located below the inflow of the lower disk causing a gradient that drove the flow (in the upwards direction) through the sample. The inflow and outflow reservoir of the disks were located 4 cm apart with the lower disk inflow tube even with the bottom of the core to start (i.e., the outflow of the upper disk was located 4 cm below the bottom of the sample which generated a pressure (ψ)), to produce a hydraulic gradient of 0.8 cm cm^{-1} (4 cm head change/5 cm core height). Water discharged per unit time was measured from the outflow of the upper disk and Darcy's law was used to calculate K (hydraulic conductivity = discharge/gradient \times cross sectional area). The in- and outflow of the disks were then lowered further (but still 4 cm apart) so that the gradient remained the same but the pressure (ψ) decreased. This was repeated for ψ of approximately -4, -8, -12, -16, -20 and -24 cm of water.

The same tension disks were used for retention experiments by placing the cores on top of a single covered disk and lowering the outflow of the disk. Once the water had stopped draining from the core the outflow tube was lowered and the process repeated. The outflow tube was positioned below the sample to produce ψ of at -0.5, -4, -8, -12 and so on in ~ 4 cm increments to about -40 cm of water. The process was repeated in reverse allowing the core to re-saturate. The cores were weighed before and after each level of pressure so that the volumetric moisture content (θ) could be determined gravimetrically once the cores were dried. In dual porosity media it is useful to differentiate between mobile (available for drainage and flow) and immobile (e.g., water in hyaline cells) water contents (c.f. Nielsen et al., 1986). Here, we use θ_r to represent the residual water content which is equivalent to the immobile water under the range of ψ used (since the pressure would not be sufficient to drain the hyaline cells of *Sphagnum* mosses).

Saturated hydraulic conductivity (K_{sat}) was determined using a permeameter experiment. Due to the fragile and very porous nature of the core there was concern of preferential flow along the side of the permeameter, artificially increasing discharge (and thus K). Using wax (Hoag and Price, 1995) or gypsum slurry (Beckwith et al., 2003) to encapsulate the core was ruled out because of concern that the material would infiltrate the very porous sample, reducing the effective porosity (and lowering K). To mitigate preferential flow a flexible (latex) liner was affixed along the inside wall of a Plexiglas cylinder which was slightly larger than the diameter and height of the core. The core was inserted into the latex lined Plexiglas cylinder and rested on a perforated Plexiglas disc at the bottom. A syringe filled with water was inserted into the latex lining and water was injected causing the lining to swell, cuddling the core and reducing any preferential vertical flow paths along the side of the core. The bottom of the cylinder was con-

nected to a water source and water was pushed through the core upwards. A drain at the top of the cylinder allowed the measurement of discharge and the height difference between the inflow source and the drain determine the gradient.

Model simulation with HYDRUS 1D and RETC

RETC was used to predict the moisture profile for experiment 1 and HYDRUS 1D version 4.05 (Simunek and Sejna, 1999) was used to simulate transient moisture content for experiments 2 and 3. HYDRUS numerically solves Richard's Equation for variably saturated flow. For all experiments the hydraulic parameters were based on measurements as described above. K was expressed as a function of ψ , and both $\theta(\psi)$ and $K(\psi)$ were fitted using the RETC code of van Genuchten et al. (1991) for single-porosity soil. RETC was run with the empirical constant $m = 1 - 1/n$ (van Genuchten, 1980); simultaneous fitting of hydraulic conductivity (Mualem, 1976) and water retention data (i.e., the hydraulic functions noted above). In the model simulations the initial condition was specified in terms of ψ , by setting the wt to $\psi = 0$ cm of water at the requisite level, and assuming an equilibrium profile to the surface and to the bottom of the sample. At each level the initial θ condition was thus a function of the θ - ψ relation. In experiment 1 the wt ($\psi = 0$) was lowered sequentially. At each stage θ was determined using the new pressure distribution and RETC. In experiment 2 the lower boundary had a specified flux, and the surface was specified as a no-flow boundary. In experiment 3 the lower boundary was no-flow, and the upper boundary was a specified flux boundary based on the measured average evaporation. Variable time-stepping was used.

Results

Hydraulic properties of the *Sphagnum* profile

Water retention curves for the *Sphagnum* profile show a distinct pattern in which the upper layers of moss undergo a greater range of drying and wetting for an equivalent change in pressure, compared to mosses from deeper in the profile (Fig. 1). The saturated water contents (θ_s) were all similar, and ranged from 0.87 to $0.92 \text{ cm}^3 \text{ cm}^{-3}$. There was considerable hysteresis (see also Hayward and Clymo, 1982). In the upper moss section (5 cm) the greatest difference between wetting and drying θ was in the highest pressure range (-10–0 cm). In lower sections there was an appreciable difference with drying θ up to $0.1 \text{ cm}^3 \text{ cm}^{-3}$ greater

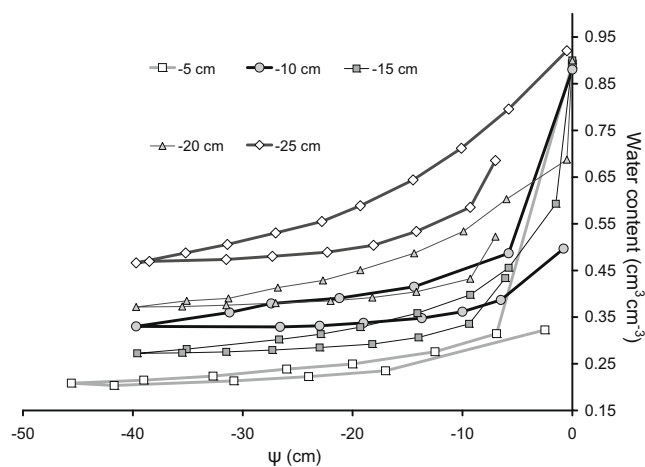


Fig. 1. Water retention curves for drainage and rewetting of mass samples.

in all samples, for a given pressure. The drying portion of the retention curves fitted well with van Genuchten parameters using the RETC code (Table 1). More detailed results on some of the samples are provided by Price et al. (2008).

The hydraulic conductivity (K) versus pressure (ψ) relation, $K(\psi)$, also varied distinctly with depth in the profile (Fig. 2). In the upper layer (5 cm) the saturated hydraulic conductivity ($K_{\psi=0 \text{ cm}}$) was highest ($1.8 \times 10^{-3} \text{ m s}^{-1}$), but with a decline in pressure to $\psi = -25 \text{ cm}$, hydraulic conductivity was reduced the most ($K_{\psi=-25 \text{ cm}} = 4 \times 10^{-8} \text{ m s}^{-1}$). In comparison deeper moss samples had lower saturated hydraulic conductivity and higher unsaturated hydraulic conductivity at a given pressures ($K_{\psi=0 \text{ cm}} = 2.3 \times 10^{-4}$ and $K_{\psi=-25 \text{ cm}} = 1.1 \times 10^{-5} \text{ m s}^{-1}$), thus a smaller range corresponding to the smaller range of θ at depth.

Bucket experiments

The dielectric constant reported by the TDR100 system was converted to water content values using the following empirical (Kellner, E. personal communication) relationship for moss samples: $\theta = 0.039 + 0.0317 \text{ Ka} - 0.00045 \text{ Ka}^2 + 0.0000026 \text{ Ka}^3$, where Ka is the dielectric constant determined from the travel time of the electromagnetic wave generated by the TDR on the soil.

The stepped drainage experiment (experiment 1) showed a rapid and stable response to both drainage and wetting (Fig. 3). The water content at the initial condition when wt was at -10 cm was at or near saturation for all but the 5 cm depth, ranging from 0.85 to $0.88 \text{ cm}^3 \text{ cm}^{-3}$. Water content in each sensor decreased sequentially as wt dropped below it. In the most drained condition (day 13) water content approached but remained above the residual water content. Reversing the drainage (refilling) resulted in sequential rise in θ at each unsaturated layer. Careful inspection of Fig. 3, however, reveals that returning wt to the set level did not result in rewetting to the same level as drainage for any sensor. For example, $\theta_{-5 \text{ cm}}$ recovered to 0.41 from $0.48 \text{ cm}^3 \text{ cm}^{-3}$; $\theta_{-10 \text{ cm}}$ returned to 0.42 from 0.55 in the step when the water table drops from -15 to -20 cm , then back to -15 cm . Fig. 4 shows profiles of θ at each stage of water table after a stable θ was reached. Note that θ approaches the residual water content (θ_r) in the upper layers (5 and 10 cm depth) when wt was 25 cm below the surface (i.e., $\theta_{-5 \text{ cm}}$ and $\theta_{-10 \text{ cm}}$ were similar with wt 25 and 30 cm below the surface). Note also there is evidence of greater capillary retention at 25 cm depth (convex lower portion of the curve when wt was 30 cm below the surface).

In experiment 2, evaporation was not allowed and the controlled continuous basal seepage of $\sim 0.7 \text{ cm d}^{-1}$ produced a water table drop of $\sim 1.5 \text{ cm d}^{-1}$ (Fig. 5). The water table was initially at -10.9 cm and dropped to -33.9 cm by day 15 and seepage was stopped for the duration of the experiment (day 17). The θ was initially at saturation (θ_s) for all depths but at the 5 cm depth. There, $\theta_{-5 \text{ cm}}$ was initially $0.4 \text{ cm}^3 \text{ cm}^{-3}$ and fell gradually but steadily to

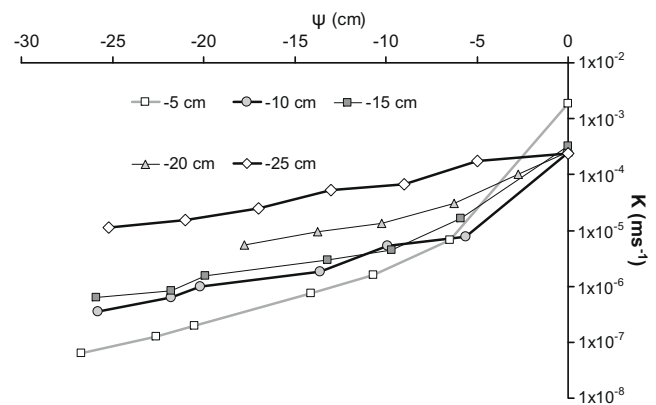


Fig. 2. Hydraulic conductivity versus pressure from measured data.

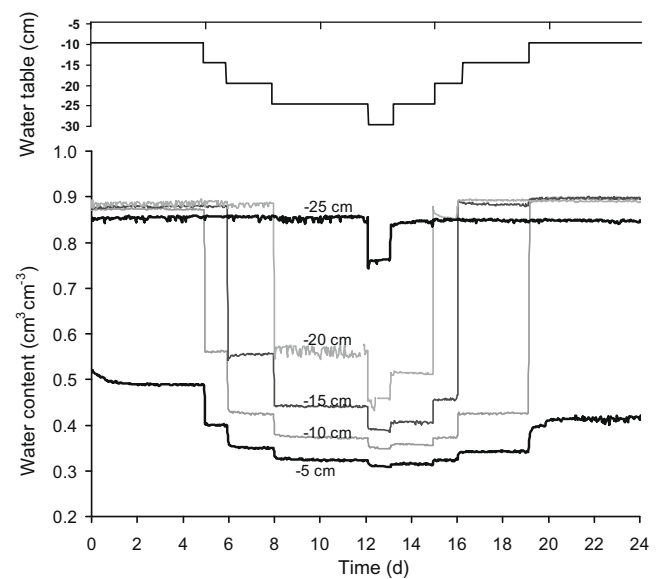


Fig. 3. Experiment 1, staged water table (wt) decline: upper graph shows stages of wt manipulation. Lower graph shows volumetric water content (θ) measured at -5 , -10 , -15 , -20 and -25 cm below the surface as wt was lowered.

$0.28 \text{ cm}^3 \text{ cm}^{-3}$ over the experiment (Fig. 5). At deeper points, $\theta_{-10 \text{ cm}}$, $\theta_{-15 \text{ cm}}$, $\theta_{-20 \text{ cm}}$ and $\theta_{-25 \text{ cm}}$, saturation was maintained until day 0, 3, 7 and 11, respectively, thereafter declining to a fairly constant θ . With wt at -25 cm , the minimum θ for the 5, 10, 15, 20 and 25 cm layer was 0.28, 0.32, 0.33, 0.38 and $0.68 \text{ cm}^3 \text{ cm}^{-3}$, respectively. Apparently $\theta_{-5 \text{ cm}}$ ($0.29 \text{ cm}^3 \text{ cm}^{-3}$) was not at the measured residual water content, θ_r ($0.21 \text{ cm}^3 \text{ cm}^{-3}$) (Fig. 1 and Table 1), although $\theta_{-10 \text{ cm}}$, $\theta_{-15 \text{ cm}}$ and $\theta_{-20 \text{ cm}}$, were generally

Table 1
Physical, hydraulic and RETC curve-fitting parameters of the $\sim 5 \text{ cm}$ layers of *Sphagnum* hummock. Curve-fitting parameters were estimated with RETC using both $\theta(\psi)$ and $K(\psi)$. RETC was run with the empirical constant $m = 1 - 1/n$; simultaneous fitting of hydraulic conductivity (weighting 0.8) and water retention data (Van Genuchten et al., 1991) and θ_r set to 0.02 at -15 m pressure (Boelter, 1968).

Depth ^a (cm)	ρ_B (g cm^{-3})	θ_s (cm^3)	θ_r (cm^{-3})	α^b	n^b	L^c	K_s ($\times 10^{-5} \text{ m s}^{-1}$)	$K_{(\psi=-25)}$ ($\times 10^{-5} \text{ m s}^{-1}$)
-5	0.04	0.89	0.2	10.18	1.25	-4.38	183	0.004
-10	0.034	0.87	0.33	0.27	1.47	-1.86	24.5	0.037
-15		0.92	0.27	0.53	1.57	-2.51	31.9	0.063
-20	0.038	0.9	0.37	0.38	1.38	-1.31	33.1	0.37
-25		0.93	0.47	0.27	1.28	-1.81	23.5	1.11

^a Mid-depth of 5 cm samples.

^b n are empirical constants that affect the shape of the (predicted) water retention curve.

^c L is a parameter in Mualem's model that accounts for pore tortuosity and connectivity.

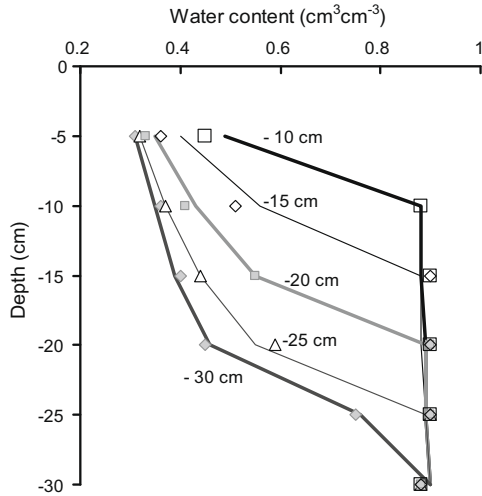


Fig. 4. Experiment 1, staged water table (wt) decline: volumetric water content (θ) profiles as wt was lowered from -10, -15, -20, -25 and -30 cm. The point measurements are the simulated values for the respective profiles they touch or almost touch (e.g., white diamonds and thick black line represent the wt at -15 cm profile).

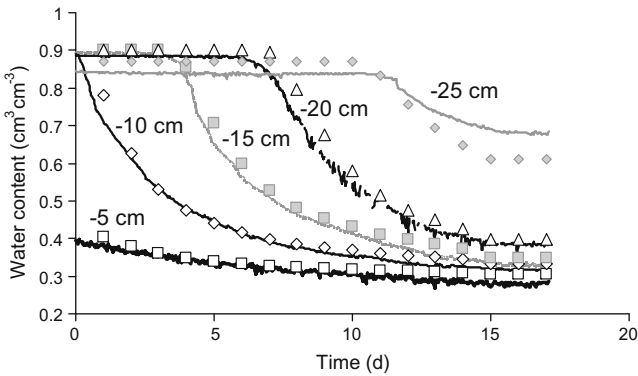


Fig. 5. Experiment 2, continuous drainage: line data represent continuous (TDR100) data for the probe located at that depth. Point (symbols) data are the modelled values, approximating the respective continuous line data (e.g., grey square is -15 cm, while triangle -20 cm).

closer to their respective θ_r , while $\theta_{-25\text{ cm}}$ at $0.68\text{ cm}^3\text{ cm}^{-3}$ remained well above its θ_r ($0.47\text{ cm}^3\text{ cm}^{-3}$).

In experiment 3 there was no basal seepage but the surface was left uncovered to allow evaporation for 34 days. The average evaporation rate was 3.2 mm d^{-1} , but for the first 6 days was greater (average 4.7 mm d^{-1}), than the remaining 24 days (average 2.2 mm d^{-1}) (Fig. 6a). Correspondingly, wt dropped at 1.1 cm d^{-1} during the initial period, but thereafter averaged 0.5 cm d^{-1} , descending from 9.5 to 30.1 cm below the surface over the experiment. Water content at -5 cm ($\theta_{-5\text{ cm}}$) began at $0.45\text{ cm}^3\text{ cm}^{-3}$ and dropped to $0.4\text{ cm}^3\text{ cm}^{-3}$ after one day, then declined steadily to $0.31\text{ cm}^3\text{ cm}^{-3}$ over the experiment (Fig. 6b). Also $\theta_{-10\text{ cm}}$ dropped quickly at first ($0.32\text{ cm}^3\text{ cm}^{-3}$ in 2 days). The next three layers, $\theta_{-10\text{ cm}}$, $\theta_{-15\text{ cm}}$ and $\theta_{-20\text{ cm}}$, reached $0.4\text{ cm}^3\text{ cm}^{-3}$ after 16, 30 and 39 days, respectively, whereas $\theta_{-25\text{ cm}}$ reached a minimum of $0.67\text{ cm}^3\text{ cm}^{-3}$ by the end of the experiment. Saturated water content was sustained in $\theta_{-15\text{ cm}}$, $\theta_{-20\text{ cm}}$ and $\theta_{-25\text{ cm}}$ for 4, 14 and 30 days, respectively. Note that $\theta_{-25\text{ cm}}$ decreased steadily from 0.85 to $0.81\text{ cm}^3\text{ cm}^{-3}$ from the beginning of the experiment to day 30, when a more abrupt change occurred.

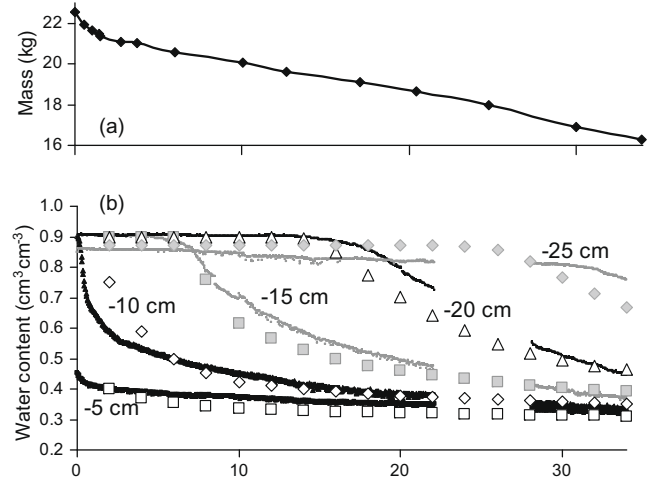


Fig. 6. Experiment 3, evaporation: upper graph (a) shows the mass of the bucket over time. Lower graph (b) shows line data that represents continuous (TDR100) data for the probe located at that depth. Point (symbols) data are the modelled values, approximating the respective continuous line data (e.g., grey square is -15 cm, while triangle -20 cm). The gap in the data between day 22 and 27 was due to a power failure in the logger.

Modeling

In simulation 1, RETC parameters were used to derive the distribution of θ for each water table depth and the resulting values were plotted against the measured θ distribution (Fig. 4). The RETC-derived θ fit the data well (Fig. 4). The θ versus depth profile gets steeper as wt drops, and θ in the upper layers gets progressively drier. This, along with the non-zero slopes at lower pressures in Fig. 1 suggests θ_r has not been fully achieved at any level.

HYDRUS 1D was run two times to simulate experimental data, identified below as simulation 2 and 3. In simulation 2, the initial condition was reset so $\psi = 0$ at -10 cm depth with the pressure at equilibrium throughout the sample, and basal seepage at the specified flux (0.7 cm d^{-1}). The simulation with HYDRUS 1D provided an excellent fit for all depths except $\theta_{-25\text{ cm}}$, which while predicting the timing of the decline in θ , overestimated the decline by $0.07\text{ cm}^3\text{ cm}^{-3}$ by the end of the experiment (see Fig. 5).

In simulation 3 the initial conditions were again reset as in simulation 2. The evaporation flux at the upper boundary was set to represent the two phases of evaporation noted previously, with evaporation averaging 4.7 mm d^{-1} for the first 6 days, and 2.2 mm d^{-1} thereafter. With the exception of the 10 cm layer, the simulated decline in θ was more rapid than the observed values (Fig. 6b), but the timing of the initial decrease matched reasonably well except for the 25 cm layer. At $\theta_{-25\text{ cm}}$ the fit was poor. HYDRUS did not predict the slow decline in θ prior to day 30, under-predicted the timing of the more abrupt drainage on day 30 and under-predicted the measured value.

Discussion

Water retention properties reflect the decreasing characteristic pore size that occurs with depth in a moss profile. Moss from the surface layer had retention properties very similar to those reported by Boelter (1968, 1969) for live undecomposed moss, with $\theta_s \sim 0.9\text{ cm}^3\text{ cm}^{-3}$, most of the water draining out at any pressure below zero (air-entry pressure essentially zero) and dropping to $0.25\text{ cm}^3\text{ cm}^{-3}$ at $\psi_{-15\text{ cm}}$, and $\theta_r \sim 0.2$. Here, between $\psi_{0\text{ cm}}$ and $\psi_{-6.5\text{ cm}}$ 70% of the water in the sample drained. The equivalent pore-diameter ($2r$), based on the relation $2r = 3000/\psi$ (McLay

et al., 1992) at $\psi_{-6.5 \text{ cm}} = \sim 0.5 \text{ mm}$, demonstrates the inability of *Sphagnum* to retain water in the larger active pores in the matrix, and moreover their predominance in the upper layer. The consequence was a two order of magnitude drop in K , from 10^{-3} to 10^{-5} m s^{-1} (Fig. 2). The inability of the undecomposed mosses to hold water in the primary interstitial pores greatly increases the flowpath tortuosity in peat as the air-filled pores coalesce (Quinton et al., 2009), resulting in low hydraulic conductivity in all but saturated conditions, uncommon at the surface of hummocks. With the water table in hummocks typically 40 cm or more below the hummock surface (e.g., Yazaki et al., 2006), and assuming an equilibrium pressure distribution, $K(\psi_{-40 \text{ cm}})$ drops to 10^{-8} m s^{-1} (Fig. 2). In other words, when the water table is 40 cm below the hummock surface, the water flux becomes severely constrained by the low hydraulic conductivity, and capillary rise may be insufficient to sustain evaporation (Price, 1991).

Below 40 cm the pore size distribution contained sufficiently small pores to retain water ($\theta_r > 0.3 \text{ cm}^3 \text{ cm}^{-3}$) and result in a higher $K(>10^{-6} \text{ m s}^{-1})$ (Figs. 1 and 2). The higher water content of the lower layers, combined with the relative mobility of water there (higher K), suggests lower layers are an important water store that can easily supply water to the upper layers when the demand is there and the hydraulic gradients are sufficient (cf. Schouwenaars and Gosen, 2007). In the drainage and evaporation experiments the water content of the upper layer varied little, generally between $0.3\text{--}0.4 \text{ cm}^3 \text{ cm}^{-3}$. It was well drained when wt was high, and apparently well supplied with water when wt was low. Alternatively, the lower layers experienced a greater range of θ as wt descended, due to the presence/absence of the water table within this zone. A similar pattern was described from field data in hummocks by Yazaki et al. (2006), where θ was relatively constant in the top layer (which remained unsaturated) but more variable at depth. Thus despite large water table fluctuations below, the steep $K(\psi)$ curve exerts a stabilizing influence on moisture content in the top layer.

In experiment 1 lowering of wt was accompanied by a nearly instantaneous reduction of pressure to a base level θ associated with that water table, that more-or-less held constant until the next water table drop (Fig. 3). That is, at each stage of water table lowering, and at all monitored layers, pore drainage was quick, reflecting the rapid initial drop displayed in the retention curves (Fig. 1). The median pore size of undecomposed mosses is large (Quinton et al., 2009) offering little capacity for water retention. Furthermore, water that is retained may substantially be unavailable for drainage or flow since it is locked in the hyaline cells (Hayward and Clymo, 1982). This is essentially the “immobile” water in the matrix (c.f. Nielsen et al., 1986). Hoag and Price (1997) demonstrated the active porosity (i.e., excluding hyaline and dead-end cells) in poorly decomposed *Sphagnum* moss ranged from about 0.6 near the surface to 0.12 at 60 cm depth, whereas the total porosity varied from 0.9 to 0.8 over the same depth range. Accordingly, much of the water retained in drained mosses does not contribute to the flow, but remains in storage until pressures are reduced to about -100 cm of water (Hayward and Clymo, 1982); much lower than observed here. The water in the active pores, however, is easily removed by gravitational drainage. In Fig. 3 the increase in θ during the stepped water table increase was also abrupt, although the more rounded “shoulders” of the θ curve indicates a diminishing rate of water flow into the pores before equilibrium θ is reached. The hysteresis in θ on rewetting was probably associated with the inclusion of air-bubbles in active pores upon rewetting, since the hyaline cells do not drain at pressures observed here.

Simulation 1 replicated the observed θ (Fig. 4). It worked well for drainage in the range of pressures tested, although it may not perform as well in a range of pressure associated with drainage of hyaline cells (-100 cm of water).

Experiment 2 replicated basal drainage of 0.3 mm h^{-1} . In a field setting basal drainage is similarly constant. The accuracy of the simulated θ for the 5, 10, 15 and 20 cm layers was excellent (Fig. 5), especially considering the parameters were not optimized to improve the fit. The poorer match between simulated and measured θ in the 25 cm layer was in part due to the difference between θ_s determined in the retention experiments ($0.93 \text{ cm}^3 \text{ cm}^{-3}$) and the actual starting water content of the experiment ($0.85 \text{ cm}^3 \text{ cm}^{-3}$), possibly caused by incomplete rewetting of the basal layer compared to that achieved in the sectioned core used in the retention experiments, or due to compression. However, simulated θ after 11 days decreased faster than the observed θ . A possible explanation for this is that compression of the deeper layers caused by an increase in effective stress associated with decreased ψ (Price, 2003), may have resulted in a decrease of air-filled porosity (hence higher θ).

In experiment 3 a drop in the evaporation rate occurred with declining water table (Fig. 6). This has also been observed in field settings (e.g., Lafleur et al., 2005). The drop in $\theta_{-5 \text{ cm}}$ from 0.9 to $\leq 0.5 \text{ cm}^3 \text{ cm}^{-3}$ produced more than an order of magnitude decrease in hydraulic conductivity (Fig. 2), which curtails the upward flux of water that controls evaporation. At all depths the simulated θ declined more slowly than the measured ones, even though we represented the higher evaporation in the first 6 days with an average value of 4.7 mm d^{-1} , compared to 2.2 mm d^{-1} thereafter (Fig. 6a). We note that the evaporation rate declined rapidly over this 6 day period, although the accuracy and frequency of our data were insufficient to confidently increase the temporal resolution of the specified boundary flux (evaporation) rate. The inaccurate or overly-simplistic boundary condition reduced the goodness-of-fit between measured and simulated θ in the early stages of simulation. It is also possible that poor parameterization or inaccurate representation of other processes in the model reduced the fit. However, given the generally good fit of simulation 2, the parameterization is probably reasonable, so the possibility of confounding processes must be explored.

The duration of experiment 3 was about twice that of experiment 2, and over the course of experiment 3 there is a visible decrease in $\theta_{-25 \text{ cm}}$ (about $0.05 \text{ cm}^3 \text{ cm}^{-3}$) before pore drainage occurs (Fig. 6). Either this is due to the accumulation of biogenic gases in the pores (Kellner et al., 2005) which can substantially reduce hydraulic conductivity in the otherwise saturated peat (Beckwith and Baird, 2001); or it is due to consolidation of the peat which also reduces hydraulic conductivity (Price, 2003). Given the systematic decline in water table and resulting increase in effective stress on all layers, we suspect the latter. In any case, a decreasing hydraulic conductivity would cause the system to reduce the upward water flux over that predicted in the simulation based on a fixed unsaturated hydraulic conductivity function, $K(\psi)$, as seen in Fig. 2. The effect is propagated through the simulation – which over-predicts the flux into the adjacent (above) layer and eventually out of the system. This may be partially offset by the potential increase in unsaturated hydraulic conductivity of any overlying layers that experience consolidation, as the effect would be to reduce the air-filled porosity as previously explained.

Conclusion

The saturated hydraulic conductivity in *Sphagnum rubellum* is very high ($\sim 10^{-3} \text{ m s}^{-1}$), and even higher in the topmost layer (Fig. 1). However, the upper layers are rarely (if ever) saturated, and thus the unsaturated hydraulic conductivity is more relevant. Because of the large pore sizes drainage is rapid, so the unsaturated hydraulic conductivity decreases by about five orders of magnitude in the upper portion (Fig. 2). This imparts considerable restriction

to water flow. However, under steady evaporation (i.e., without irrigation or wetting from above) the mosses can sustain a water content near θ_r for an extended period, from which we can conclude the capillary transport remains efficient. Water is supplied to the surface of the hummock by upward transport from lower layers, which contain from 0.4 to 0.7 cm³ cm⁻³ of available water. In the experiments here, there was never any shortage of water to sustain evaporation (averaging 3.2 mm d⁻¹) over a 34 day period. In natural settings mosses can desiccate when evaporative demand exceeds upward transport (Ingram, 1983), before water stored in hyaline cells enters the primary (active) pore network to contribute to the upward flux. In this experiment we planned to monitor a rewetting event representing rainfall, but damage to the samples caused by transporting them from our field station to the Wetlands Hydrology Laboratory at the University of Waterloo meant we could not re-establish baseline wetness conditions, so comparison with other experiments would be fruitless. However, we recognize that water recharge from precipitation can be retained significantly by the moss capitulum, and small rain events may have no measurable effect on the water table (Strack and Price, 2009). Nevertheless, most of the time in the field setting the water content in mosses is dominated by the drained condition, and our experiments and simulations represented these well. Further experimentation to carefully monitor and then simulate rewetting by “rainfall” is needed.

For the drainage, and evaporation experiments, the capillary water flux was modelled using HYDRUS 1D in a single-porosity medium based on measured hydraulic parameters. Water loss by drainage was simulated relatively well without optimization. Water loss by evaporation was simulated moderately well for the 5–20 cm layers, but with a relatively small systematic underestimation of θ . It is possible that the hydraulic parameters (especially hydraulic conductivity) did not behave as specified with the $K(\psi)$ function, because of peat consolidation that accompanied the water table decline. In the unsaturated condition, shrinkage of the moss also occurs upon drying (Price et al., 2008). This has the effect of increasing θ by shrinking the soil volume for a given volume of water. Shrinkage and consolidation were not accounted for in this study.

We believe this is the first application of a 1D numerical model to model water flow in undecomposed mosses using measured parameters and verified using real data. The results suggest the appropriateness of using the Mualem–van Genuchten model for fitting hydraulic parameters in non-moisture limiting conditions. The success of this modelling is encouraging, and demonstrates its utility for evaluating the ability of mosses to sustain critical levels of wetness under moderate evaporation and drainage conditions. Further experimentation and modelling are required to explore a greater range of environmental conditions, including rewetting from above (rain) and drying beyond the θ_r caused by drainage so that water in hyaline cells is considered.

Acknowledgements

We thank the Natural Science and Engineering Council (NSERC) of Canada for financial assistance; Erica Faux for help with the measurement of hydraulic parameters; and James Craig for helpful comments on the manuscript. We also thank Jean Caron for helpful discussions in the design of the apparatus to test unsaturated hydraulic conductivity. We also thank two anonymous reviewers for their insightful comments.

References

Beckwith, C.W., Baird, A.J., 2001. Effect of biogenic gas bubbles on water flow through poorly decomposed blanket peat. *Water Resources Research* 37 (3), 551–558.

- Beckwith, C.W., Baird, A.J., et al., 2003. Anisotropy and depth-related heterogeneity of hydraulic conductivity in a bog peat. I: laboratory measurements. *Hydrological Processes*, 17: 89–101.
- Boelter, D., 1968. Important physical properties of peat materials. Third international peat congress, Quebec, Canada, Department of Energy, Mines and Resources and National Research Council of Canada.
- Boelter, D.H., 1969. Physical properties of peats as related to degrees of decomposition. *Soil Science Society of America Journal* 33, 606–609.
- Clymo, R.S., 1970. The growth of *Sphagnum*: methods and measurement. *Journal of Ecology* 58, 13–40.
- Clymo, R.S., 1983. Peat. In: Gore, A.J.P. (Ed.), *Ecosystems of the World 4a: Mires: Swamp, Bog, Fen and Moor*. Elsevier Scientific Publishing Company, New York, pp. 159–224.
- Clymo, R., 1984. The limits to peat bog growth. *Philosophical transactions of the Royal Society of London, series B. Biological Sciences (1934–1990)* 303 (1117), 605–654.
- Clymo, R., Hayward, P., 1982. The ecology of *Sphagnum*. *Bryophyte Ecology*, 229–289.
- Gunnarsson, U., Rydin, H., 2000. Nitrogen fertilization reduces *Sphagnum* production in bog communities. *New Phytologist* 147 (3), 527–537.
- Hayward, P., Clymo, R., 1982. Profiles of water content and pore size in *Sphagnum* and peat, and their relation to peat bog ecology. *Proceedings of the Royal Society of London, series B (1934–1990). Biological Sciences* 215 (1200), 299–325.
- Hoag, R.S., Price, J.S., 1995. A field-scale, natural gradient solute transport experiment in peat at a Newfoundland blanket bog. *Journal of Hydrology* 172, 171–184.
- Hoag, R.S., Price, J.S., 1997. The effects of matrix diffusion on solute transport and retardation in undisturbed peat in laboratory columns. *Journal of Contaminant Hydrology*, 28.
- Ingram, H.A.P., 1978. Soil layers in mires – function and terminology. *Journal of Soil Science* 29 (2), 224–227.
- Ingram, H.A.P., 1983. Hydrology. In: Gore, A.J.P. (Ed.), *Ecosystems of the World: Mires: Swamp, Bog, Fen and Moor, vol. 4A*. Elsevier Scientific Publishing Company, New York, pp. 67–158.
- Kellner, E., Waddington, J.M., Price, J.S., 2005. Dynamics on biogenic gas bubbles in peat: Potential effects on water storage and peat deformation. *Water Resources Research* 41, W08417. 12p.
- Kuhry, P., Vitt, D., 1996. Fossil carbon/nitrogen ratios as a measure of peat decomposition. *Ecology* 77 (1), 271–275.
- Lafleur, P., Hember, R., et al., 2005. Annual and seasonal variability in evapotranspiration and water table at a shrub-covered bog in Southern Ontario, Canada. *Hydrological Processes* 19 (18), 3533–3550.
- Luken, J., 1985. Zonation of *Sphagnum* mosses: interactions among shoot growth, growth form, and water balance. *The Bryologist* 88 (4), 374–379.
- McLay, C., Allbrook, R., et al., 1992. Effect of development and cultivation on physical properties of peat soils in New Zealand. *Geoderma (Amsterdam)* 54 (1–4), 23–37.
- McNeil, P., Waddington, J., 2003. Moisture controls on *Sphagnum* growth and CO₂ exchange on a cutover bog. *Journal of Applied Ecology* 40 (2), 354–367.
- Mualem, Y., 1976. A new model for predicting the hydraulic conductivity of unsaturated porous media. *Water Resources Research* 12, 513–522.
- Nielsen, D.R., van Genuchten, M., et al., 1986. Water flow and solute transport processes in the unsaturated zone. *Water Resources Research* 22, 895–108S.
- Price, J., 1991. Evaporation from a blanket bog in a foggy coastal environment. *Boundary-Layer Meteorology* 57 (4), 391–406.
- Price, J.S., 2003. Role and character of seasonal peat soil deformation on the hydrology of undisturbed and cutover peatlands. *Water Resources Research* 39 (9), 1241.
- Price, J., Whittington, P., et al., 2008. A method to determine unsaturated hydraulic conductivity in living and undecomposed *Sphagnum* moss. *Soil Science Society of America Journal* 72 (2), 487.
- Price, J.S., Edwards, T.W.D., et al., 2009. Physical and isotopic characterization of evaporation from *Sphagnum* moss. *Journal of Hydrology* 396 (1–2), 175–182.
- Quinton, W.L., Elliot, T., et al., 2009. Measuring physical and hydraulic properties of peat from X-ray tomography. *Geoderma* 153, 269–277.
- Rezanezhad, F., Quinton, W.L., et al., 2009. Examining the effect of pore size distribution and shape on flow through unsaturated peat using computer tomography. *Hydrology and Earth System Sciences* 13, 1993–2002.
- Rochefort, L., Vitt, D., et al., 1990. Growth, production, and decomposition dynamics of *Sphagnum* under natural and experimentally acidified conditions. *Ecology* 71 (5), 1986–2000.
- Sagot, C., Rochefort, L., 1996. Tolérance des sphaignes à la dessiccation. *Cryptogamie. Bryologie, lichénologie* 17 (3), 171–183.
- Schipperges, B., Rydin, H., 1998. Response of photosynthesis of *Sphagnum* species from contrasting microhabitats to tissue water content and repeated desiccation. *New Phytologist* 140 (4), 677–684.
- Schouwenaars, J., Gosen, A., 2007. The sensitivity of *Sphagnum* to surface layer conditions in a re-wetted bog: a simulation study of water stress. *Mires and Peat*, 2.
- Simunek, J., Sejna, M. et al. 1999. The HYDRUS-2D software package for simulating two-dimensional movement of water, heat, and multiple solutes in variably saturated media. version 2.0. Rep. IGWMC-TPS 53, 251.
- Strack, M., Price, J.S., 2009. Moisture controls on carbon dioxide dynamics of peat-*Sphagnum* monoliths. *Ecology* 2, 34–41.

- Strack, M., Waddington, J., et al., 2006. Response of vegetation and net ecosystem carbon dioxide exchange at different peatland microforms following water table drawdown. *Journal of Geophysical Research*, 111.
- Tolonen, K., Turunen, J., 1996. Accumulation rates of carbon in mires in Finland and implications for climate change. *The Holocene* 6 (2), 171.
- van Genuchten, M., 1980. A closed-form equation for predicting the hydraulic conductivity of unsaturated soils. *Soil Science Society of American Journal* 44 (5), 892–898.
- van Genuchten, M., Leij, F., et al., 1991. The RETC code for quantifying the hydraulic functions of unsaturated soils. In: Kerr, Robert S. (Ed.). *Environmental Research Laboratory, Office of Research and Development, US Environmental Protection Agency Ada, Okla., USA*.
- Whittington, P., Price, J.S., 2006. The effects of water table draw-down (as a surrogate for climate change) on the hydrology of a patterned fen peatland near Quebec City, Quebec. *Hydrological Processes* 20, 3589–3600.
- Yazaki, T., Urano, S.-I., et al., 2006. Water balance and water movement in unsaturated zones of *Sphagnum* hummocks in Fuhrengawa Mire, Hokkaido, Japan. *Journal of Hydrology* 319, 312–327.